A Study of Heavy Rainfall Events during the Great Midwest Flood of 1993

NORMAN W. JUNKER

Hydrometeorological Prediction Center, NCEP, Camp Springs, Maryland

RUSSELL S. SCHNEIDER

Storm Prediction Center, NSSL, Norman, Oklahoma

STEPHANIE L. FAUVER

NWS, Charleston, South Carolina

(Manuscript received 29 July 1998, in final form 24 March 1999)

ABSTRACT

A synoptic–dynamic climatology was constructed using all 24-h 2-in. (50.8 mm) or greater rainfall events in nine states affected by heavy rains and flooding from June through September 1993 using 6- or 12-h gridded analyses from the Regional Data Assimilation System and geostationary satellite imagery. Each of the 85 events was assigned a category (0–4) based on the areal coverage of the 3-in. (76.2 mm) or greater observed precipitation isohyet. A variety of meteorological fields and rules of thumb used by forecasters at the Hydrometeorological Prediction Center are investigated that may help identify the most likely location and scale of a convective precipitation event.

The heaviest rain usually fell to the north (downwind) of the axis of highest 850-mb winds and moisture flux in an area of 850-mb warm temperature and equivalent potential temperature advection. The rainfall maximum also usually occurred to the north or northeast of the axis of highest 850-mb equivalent potential temperature. The scale and intensity of the rainfall appeared to be related to 1) the magnitude of the warm advection, 2) the 1000–500-mb mean relative humidity, 3) the breadth of the axis of stronger values of moisture transport feeding northward into a surface boundary, 4) the strength of low-level moisture flux convergence, and 5) the length of the low-level moisture flux convergence that was aligned along the mean flow upstream from the location of the rainfall maximum. The latter finding suggests that propagation plays an important role in modulating the scale and intensity of rainfall events.

1. Introduction

A number of mesoscale convective systems (MCSs) contributed to the rainfall that led to the extreme flooding of the upper Mississippi and Missouri Valley region during the spring and summer of 1993 (Kunkel et al. 1994). Rainfall during the period, especially June and July, was unusually heavy with numerous locations receiving new monthly maxima (Guttman et al. 1994). For the 2-month period (June–July), the estimated return period for the observed rainfall at a number of locations was estimated to be more than 100 years (Guttman et al. 1994). By August, although the worst of the heavy rains and flooding ended for most of the Midwest and northern plains, a number of mesoscale convective systems still affected the region. September brought a dramatic decrease in convective activity until late in the month when a 4-day period of torrential rainfall led to serious flooding over portions of southeastern Kansas and southwestern Missouri. The June–September 1993 period offered the opportunity to study a number of mesoscale convective systems that were associated with heavy-to-extreme rainfall.

A number of studies have associated mesoscale convective complexes (MCCs) and systems (MCSs) with heavy rain and flash floods (e.g., Maddox et al. 1979, 1982; Maddox 1980). Fritsch et al. (1986) noted that 30%–50% or more of warm-season rainfall in the United States can be attributed to MCSs. An examination of the small-scale structure of MCC precipitation by McAnelly and Cotton (1986) indicates that most of the heavy precipitation coincides with meso-β-scale areas of intense convection. The favored region for the development of meso-β elements is along the right flank of MCCs where the strongest low-level convergence is located due to the influx of moist unstable air (Merritt

Corresponding author address: Norman W. Junker, NOAA/NWS, 5200 Auth Rd., Room 410, Suitland, MD 20746.
E-mail: norman.junker@noaa.gov

and Fritsch 1984; Bartels and Rockwood 1983; Maddox 1983).

Kane et al. (1987) used these earlier studies as a basis for speculating that MCCs may routinely produce asymmetric, but frequently similar, precipitation patterns. They then documented the average temporal and spatial characteristics of precipitation and developed a relationship between the average precipitation pattern and the satellite-observed cold-cloud shield. Mesoscale systems were classified into four categories (frontal, synoptic, mesohigh, and extreme right-moving events) and an average precipitation field was constructed for each type. Synoptic conditions for the first three of these categories were described by Maddox et al. (1979). Kane et al. (1987) noted that the final type (extreme right movers) was a subset of the frontal category, but because of the distinctive movement of the MCC with respect to the mean wind field, it was categorized separately. They found that the rainfall patterns were similar for each type, but that the size and magnitude of the precipitation varied. The larger-scale, heavy rainfall producing systems generally were synoptic and frontal type events that occurred early in the warm season when the dynamics were strongest. The scale of the precipitation was smallest in mid- and late summer with mesohigh events.

Accurately predicting the scale of convective systems is one of the most difficult tasks in forecasting. The National Oceanic and Atmospheric Administration's Disaster Survey Report of the Great Flood of 1993 noted that Hydrometeorological Prediction Center (HPC) forecasters overpredicted the areal coverage of precipitation from MCCs and MCSs during June–July 1993 (NOAA 1994). The composites developed by Kane et al. (1987) offer forecasters insight into average precipitation spatial scales for various types of MCSs. Our study was initiated to try to gain additional insight into forecasting the most likely scale, amount, and location of the heavy rainfall associated with MCSs.

The nine states affected by heavy rains and flooding from June through September 1993 were North and South Dakota, Nebraska, Kansas, Minnesota, Wisconsin, Iowa, Illinois, and Missouri. A synoptic–dynamic climatology was constructed in these nine states using all 24-h 2 in. (50.8 mm) or greater rainfall events in the 6- or 12-h gridded analyses from the Regional Data Assimilation System (RDAS) and Geostationary Operational Environmental Satellite (GOES) imagery to construct our database. Composed of 85 individual 2 in. or greater rainfall events, 43 of them being at least 5 in. (127 mm), the cases provide a unique opportunity to study the similarities and differences between the largest scale, most extreme rainfall events and other smaller-scale heavy rainfall events. The maximum rainfall, the areal coverage of the 2-, 3- (76.2 mm), 4- (101.6 mm), and 5-in. isohyets, and a variety of meteorological diagnostic fields and empirical heavy rain forecast rules were evaluated to study the synoptic–dynamic characteristics of the events.

2. Methodology

A high-density network of precipitation observations from the National Weather Service's River Forecast Centers, synoptic reports, and GOES satellite imagery were used to identify the 85 different MCSs from June through September 1993 that produced 24-h (1200 to 1200 UTC) rainfall amounts greater than 2 in. Visible, infrared, and 6.7-μm water vapor imagery were examined to determine the time of MCS initiation and decay to classify each event.

An *event oriented* approach similar to that described by Kane et al. (1987) was applied to determine the precipitation associated with each system. However, precipitation amounts were not added from two adjacent 24-h periods for those systems bridging the two periods. Instead, if a single MCS produced almost identical amounts in two 24-h periods, it was removed from the database. If a much larger rainfall amount fell during one of the adjacent 24-h periods from the same MCS, the greater of the two periods was used and the event was retained in the database. Admittedly, this methodology has drawbacks. For example, nocturnal MCSs can produce rainfall that can last past 1200 UTC; therefore, there is a distinct possibility for actual rainfall amounts from any such MCS's entire lifetime to be greater than that recorded in this study. Our methodology was used because neither hourly nor 6-hourly precipitation was available to more objectively analyze the total rainfall from each MCS. Also, subjective evaluation of satellite imagery from these events suggested that for these datasets, this approach would not produce such large analysis errors as to overly bias the study. Using satellite imagery to identify a convective system also can lead to problems since several smaller systems can merge to produce a larger one, or because one large system can split into two. When either of these scenarios occurred, precipitation from each smaller system was combined into one event.

After each event was identified, the associated area of precipitation was analyzed manually using the 24-h precipitation charts available at HPC (Olson et al. 1995). The areal coverage of the 2, 3, 4, and 5 in. or greater isohyets were then measured for each system using a planimeter.

If the centers of the heaviest rainfall from two MCSs that occurred simultaneously were within 494.4 km (240 n mi) of each other, only the system with the larger area of 2 in. or greater coverage was used. This distance was chosen arbitrarily in an attempt to ensure that an MCS that was being inhibited by a stronger one nearby was not included in the study. The rationale behind this choice was that outflow boundaries from one MCS might inhibit the flow of moist unstable air into a nearby system, especially if the more significant MCS was lo-

TABLE 1. The size criteria for the areas of 3 in. or greater precipitation that was used to define each of the precipitation categories.

Category	km^2	n mi^2
0	less than 74	less than 36
1	74–1854	36–900
2	1854–3708	901–1800
3	3709–7416	1801–3600
4	>7416	>3600

cated to the other one's south. Such a disruption to the low-level moisture inflow might therefore limit the scale and magnitude of precipitation from the ''inhibited'' MCS. If two separate areas of 3 in. or greater amounts were within the 2 in. or greater isohyet, the areal coverages of the two separate areas were added to determine the total 3-in. coverage from the MCS. The center of the isohyet representing the heaviest observed rainfall within an MCS was used as the system center. Each system identified was assigned a category (0–4) based on the areal coverage of the 3 in. or greater rainfall. Category 0 represented the smallest scale and lightest events, while category 4 events were the largest scale (Table 1). The number of cases in each category is presented in Table 2.

A database was constructed for each event using RDAS analyses (Dimego et al. 1992) that were temporally closest to the start of each event. Values of various dynamic and thermodynamic variables were computed on the original RDAS 80-km grid and their values were determined for the location of the center of each event and other grid points within 885 km of the center. Scatter diagrams then were constructed to determine which parameters were the most useful indicators of MCS development. Composites also were constructed of selected meteorological fields that appeared to have the best potential forecast value for the 12 largest scale, heavy rainfall events within the category 4 cases. These events had the largest areal coverage of 3 in. or more rainfall (Table 1) and also were associated with observed rainfall totals of 5 in. or more. Values of selected variables were interpolated from the original RDAS 80-km grid to a 9 $\times$ 9, 2° resolution latitude–longitude grid centered on the location of heaviest observed 24-h precipitation. An average value was determined for each variable on the storm-relative grid and the resultant grid was then contoured and/or plotted and normalized to a point in the center of Iowa.

In addition, a wide variety of heavy precipitation forecast rules were evaluated to identify those that might be the most useful prior to and during the development of a mesoscale convective rainfall event. The data needed to evaluate these forecast rules and assess the differences between the highest and lowest rainfall categories were entered into a spreadsheet. Scatter diagrams were also used to try to determine which factors or rules of thumb might be helpful to differentiate between categories.

TABLE 2. Number of cases, average maximum observed precipitation, and average size (km^2) of the 2, 3, 4, 5 in. or greater observed precipitation for each category.

Category	No. of cases	Max (in.)	2 in.	3 in.	4 in.	5 in.
4	15	6.7	39 057	17 918	8241	3176
3	10	6.0	17 152	5361	1728	534
2	13	5.4	12 076	3029	633	74
1	24	4.7	6253	902	136	0
0	23	2.7	1757	0	0	0
Total	85					

3. Synoptic climatology

a. Overview

Examination of the precipitation data indicates an objective method is needed to define an extreme or heavy rainfall event. Such an event can be defined by either the areal coverage of some threshold of rainfall or by the largest single amount observed during the event (Fig. 1).

Kunkel et al. (1994) noted there were a number of localized extreme events capable of producing flash floods during the period of the 1993 upper Mississippi River basin flood. Specifically, they noted 21 reports of 24-h rainfall in excess of 150 mm within the basin, a threshold they defined as extreme. We found 24 events in which the maximum observed 24-h rainfall equaled or exceeded 6 in. (152.4 mm). Inspection of satellite imagery suggested that the bulk of rain during most of these events fell in less than 6 h. The average maximum observed rainfall for our two highest categories (3 and

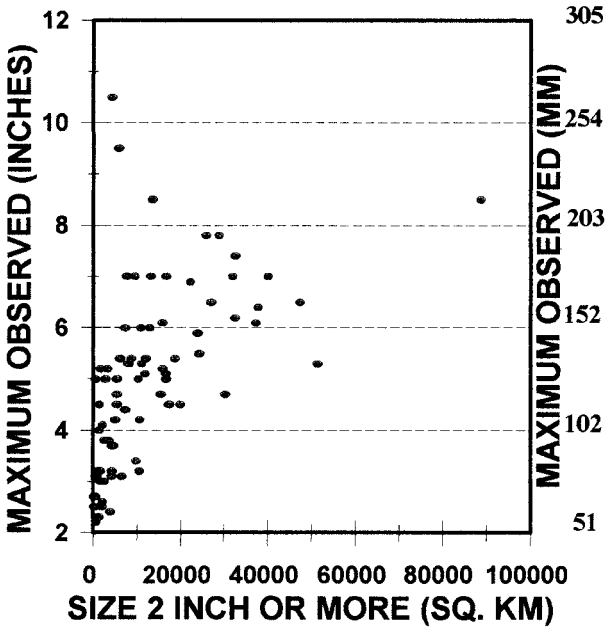

FIG. 1. Scatter diagram of the areal coverage of the 2 in. or greater rainfall versus the maximum observed rainfall for each event.

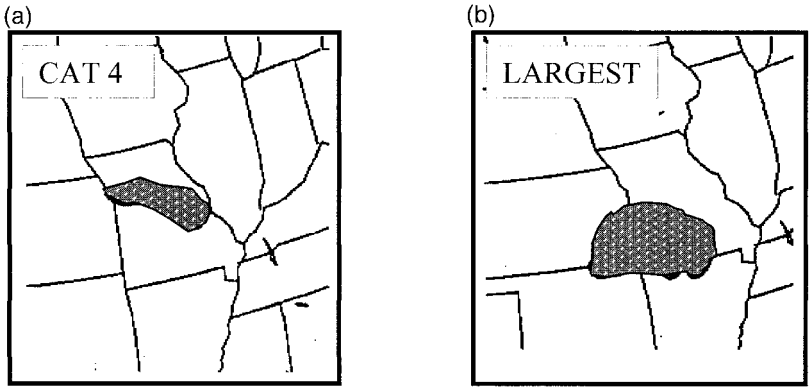

FIG. 2. (a) The median coverage of the 3 in. or greater rainfall isohyet for category 4 events, and (b) the size of the largest 3 in. or more isohyet for any case during the study.

4) was in excess of the 150 mm that was defined by Kunkel et al. (1994) as extreme. Almost all category 3 and 4 events also were associated with flash flooding. Therefore, we have altered Kunkel's definition of extreme event and henceforth define category 3 and 4 events as extreme in our study.

The scale of the heavy rainfall associated with the MCSs during this study was small. For example, the median size of the 3 in. or greater rainfall coverage, even for category 4 events, was considerably smaller than the size of Missouri (Fig. 2a). The largest 3 in. or greater coverage for any event was still significantly smaller than the size of Missouri (Fig. 2b). The core of the very heaviest rainfall was even smaller. The average 5 in. or greater coverage for category 4 events was 3176 km^2, less than one-fifth the size of the average 3-in. coverage (Table 2) for category 4 events. The 5-in. coverage for category 4 events was about the same average coverage as that for 3 in. or more for category 2 cases (Table 2). The average maximum observed precipitation

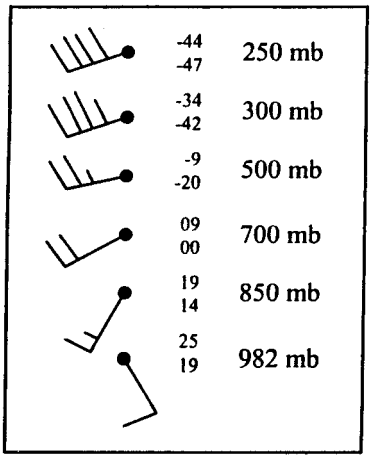

FIG. 3. Mean vertical wind, temperature, and dewpoint profile for all 2.00 in. or more cases in the dataset. Long barbs = 10 kt, short barbs = 5 kt, the top number is temperature (°C), and the bottom is dewpoint (°C).

even for category 1 and 2 events was quite high (4.7 and 5.4 in., respectively), suggesting even these lower categories are capable of producing localized flash floods. The small scale of the heaviest rainfall core makes forecasting the rainfall and flash flood potential with MCSs difficult.

The majority of rainfall events in this study, particularly the category 3 and 4 cases, shared a number of characteristics that Maddox et al. (1979) documented for frontal and mesohigh type MCSs. Common characteristics included nocturnal development with the heaviest rainfall occurring along or north of a low-level boundary in an area of low-level warm advection. More than 70% of all cases occurred between 0000 and 1200 UTC. Almost all events were associated with weak-to-moderate vertical speed shear and with winds that veered with height (Fig. 3).

Unlike the Konrad (1997) study, however, the low-level boundary for all cases in our study was usually well defined in the 850-mb equivalent potential temperature (θ_e) field. Typically, the maximum θ_e was found to the southwest of where the heaviest rainfall was observed. The heaviest rainfall also usually occurred just north of the axis of strongest southerly or southwesterly 850-mb winds and moisture flux in an area of warm and equivalent potential temperature advection which is consistent with Shi and Scofield (1987) and Juring and Scofield (1989). A much higher percentage of cases were associated with 850-mb warm temperature advection than with 500- or 300-mb positive vorticity advection.

The maximum rainfall for the majority of cases in all categories was found north of an area of relatively strong 850-mb moisture transport. This is consistent with the findings by Bell and Janowiak (1995), who noted that during the period encompassing the June–July 1993 floods, anomalously high southerly 850-mb winds and moisture transport, and strong upper-level divergence were present over the upper Midwest, a pattern favoring the formation of MCSs.

The axis of heaviest rainfall in our study usually oc-

curred within an area of 250-mb divergence but in the gradient to the south of the highest values. Approximately 60% of all cases were associated with the right entrance region of a 250-mb jet streak. However, almost 30% did not fit the divergence or convergence patterns associated with straight jet streaks described by Uccellini and Johnson (1979), suggesting that jet curvature effects should not be neglected in assessing prestorm environments (Kocin et al. 1986). About 60% of the events also were centered near the 500-mb ridge axis, another finding consistent with the Maddox et al. (1979) study.

In this section, a number of similarities have been noted between the extreme rainfall events and the less extreme ones. The similarities of the moisture and wind fields between the various categories have made forecasting precipitation associated with MCSs a great challenge. The differences found between the most (category 3 and 4) and least extreme (category 0 and 1) are often subtle, but may allow forecasters to anticipate the development of an extreme event. These differences are discussed in the next section.

b. Comparison of category 3 and 4 events with category 0 and 1 events

While the heaviest rainfall from the majority of MCSs in this study, regardless of category, occurred just north of the 850-mb moisture flux maximum, no strong correlation was found between the magnitude of the moisture flux and the rainfall category that was observed. For example, although the magnitude of the highest values of moisture flux at an MCS's center and to its south were on average greater for category 3 and 4 events, a few of the least extreme (category 0 and 1) events had magnitudes that were significantly higher than the mean values of the two highest categories.

The width of the axis of strong moisture flux appeared to be more important in differentiating between the category 0 (the lightest and smallest scale) and category 4 (the larger scale, heaviest) events. The average width of moisture flux values (18×10^{-2} m s^{-1} or higher) to the south or southwest of the category 4 events (496 km) was almost twice that of the category 0 cases (266 km). This finding is consistent with Glass and Ferry (1995), who noted that the breadth of the low-level jet appeared to play a role in determining the extent of heavy rainfall. One possible explanation is the broader axis of moisture flux into a boundary facilitates a more extensive area of moisture convergence and increases the potential for merging or training of cells. Examination of the size of the 982-mb sigma level and 850-mb moisture flux convergence indicated that typically category 3 and 4 events were associated with larger areas of strong moisture flux convergence than were lower category events.

Another difference between the category 0 and 4 events was the magnitude and depth of the moisture convergence at the location where the heaviest rain was observed. The moisture convergence was stronger through a greater vertical extent prior to and during category 4 events than with the lighter categories. For example, the layer average moisture convergence between the 982- and 896-mb sigma layers (2.98×10^{-7} s^{-1}) was almost three times greater for the most extreme events (category 4) than that for the least extreme ones (category 0, 1×10^{-7} s^{-1}). However, some individual least extreme cases were associated with stronger moisture convergence than the average value for the most extreme cases.

A number of researchers have noted that the motion of a convective system is the sum of the mean velocity of the cells making up the system and the propagation velocity due to new cells forming along the periphery of the storm (Newton and Katz 1958; Chappell 1986; Corfidi et al. 1996). Merritt and Fritsch (1984) found that the 850–300-mb mean wind vector approximates the mean cell movement within 10° during MCS genesis suggesting that when new cells form along an axis defined by the mean wind, training of cells is more likely. MCS propagation, which is very important in determining the ultimate rainfall at any one location, may slow or accelerate the system depending on which flank of the MCS is undergoing new cell formation. Slow moving or quasi-stationary MCSs may occur when the initial convection moves downstream of the area of highest instability and the axis of the low-level jet (Chappell 1986). This positions the strongest low-level moisture convergence and buoyant energy on the upstream side of the MCS where rapid new cell growth can occur (Junker and Schneider 1997). When the low-level moisture convergence is aligned upstream along the axis defined by the 850–300-mb mean wind, new cells may form and then move with the mean wind across a common location. Thus, a slow moving or quasi-stationary convective system can result as forward cell movement is negated by a backward propagation vector. These findings, therefore, suggest that one of the main differences between the most extreme (category 3 and 4) events and others should be the location and orientation of the low-level moisture convergence with respect to where the heaviest rain subsequently was observed.

To test this hypothesis, the length of the layer-average (982–896-mb sigma layers) moisture flux convergence values of 2×10^{-7} s^{-1} or greater was measured along an axis defined by the 850–300-mb mean wind but upstream of where the heaviest rainfall was observed (Fig. 4). The longer this length is along the ''average'' mean wind direction axis, the greater the potential for cell redevelopment and training and, thus, extreme rainfall amounts at the location where the maximum rainfall was observed subsequently. Category 4 events were more likely when the axis of strongest low-level moisture flux convergence was parallel to the 850–300-mb mean flow and located from 0 to 700 km upstream from where the

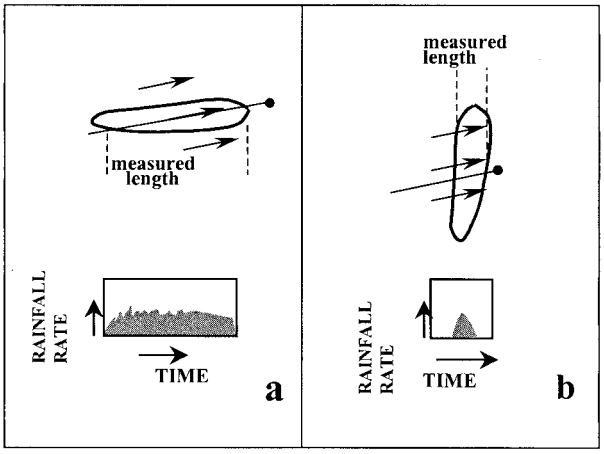

FIG. 4. Example of how the length of the moisture flux convergence was measured with respect to the mean wind upstream from the center of heaviest rainfall for (a) category 4 events and (b) category 0 events. Shown are the center of heaviest rainfall (dot), moisture flux convergence values of 2×10^{-7} s^{-1} (solid heavy line), 850–300-mb mean wind vectors (arrows), and the axis along which the moisture convergence was measured (thin line). The figure also illustrates how the rainfall intensity and duration might be affected as convection forms in the area of moisture convergence.

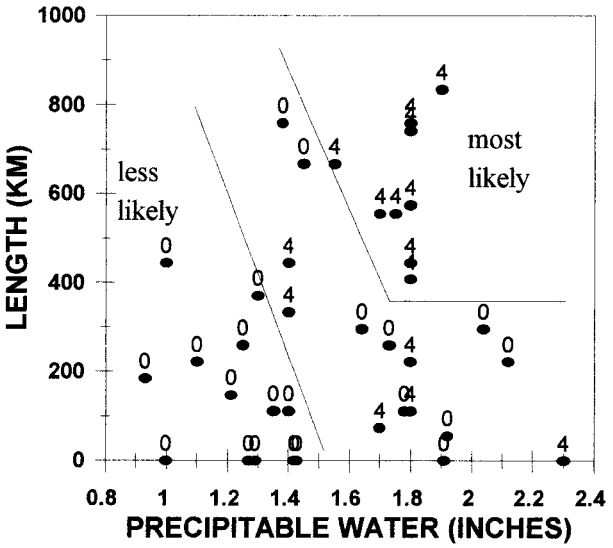

FIG. 5. Scatter diagram of the length (km) of the layer mean 2×10^{-7} s^{-1} moisture convergence of the 982- and 892-mb sigma levels (y axis) along the axis of the mean wind and precipitable water (in.; x axis). The plotted numbers are the rainfall category assigned for each event.

heaviest rainfall occurred (Fig. 4a). The length for category 4 cases averaged more than twice that of the category 0 ones. The boundary and major axis of the associated moisture convergence were more frequently aligned perpendicularly to the mean wind for the category 0 cases (Fig. 4b), resulting in lower observed rainfall. The length of the 2×10^{-7} s^{-1} or greater moisture flux convergence values along the mean wind was then plotted versus the precipitable water associated with each event within categories 0 and 4 (Fig. 5). Category 4 events were most likely when a long axis of low-level moisture convergence was oriented parallel to the direction of the mean wind and when precipitable water values were high. In these situations, new cells forming in the area of moisture convergence are likely to prolong the duration of heavy rainfall and increase ultimate rainfall amounts. Conversely, smaller-scale, lighter events (e.g., category 0) were most likely when the length of the moisture convergence oriented along the mean wind was short and when precipitable water values were low (Fig. 5).

Another subtle difference was in the 850-mb wind and moisture flux fields. The axis of strongest 850-mb winds and moisture flux appeared to migrate more slowly eastward during category 3 and 4 events than during category 0 and 1 cases. This slower eastward translation probably kept stronger low-level moisture convergence occurring longer over an area, resulting in potential cell regeneration and training over a common location and, thus, higher system rainfall amounts.

Doswell et al. (1996) noted that the magnitude of the vertical moisture flux into a convective system is one of the factors that determines the rainfall rate of the system. The broader ''tongue'' of 850-mb moisture flux and higher moisture flux convergence associated with category 4 events may give storms the potential to develop the stronger vertical moisture flux necessary to produce high rainfall rates. Doswell et al. (1996) also discussed the importance of the orientation of the convective system in determining the intensity and duration of rainfall over a given location. Our study also highlights the importance of a system's orientation and suggests that for short-range forecasts, the orientation of the moisture convergence axis with respect to the mean wind direction is an important factor in determining the scale and intensity of a convective rainfall event.

The magnitude of the 850-mb warm temperature advection was another difference between the most and least extreme MCSs. The magnitude of the warm temperature advection for category 4 events was more than twice that of the category 0 events. This argues that there was probably stronger quasigeostrophic forcing for vertical motion in association with the most extreme events.

Examination of several rules of thumb that are used by forecasters at HPC illustrates another difference between the most extreme (categories 3 and 4) and least extreme events (categories 0 and 1). Funk (1991) noted the importance of the precipitable water in assessing the rainfall potential of an MCS. He indicated that forecasters at HPC sometimes relied on a forecast technique based loosely on a study by Lowry (1972) that combined the observed or forecast 1000–500-mb thickness and precipitable water values to predict the most likely location along a boundary for organized convective development. Earlier, Swayne (1956) had defined *satu-*

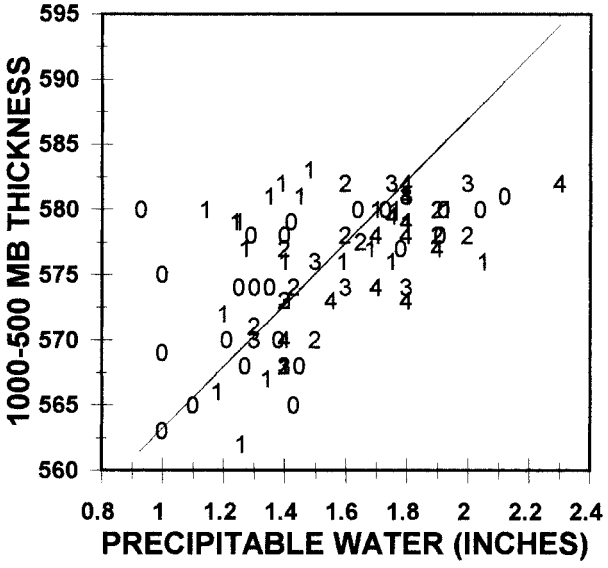

FIG. 6. Scatter diagram of precipitable water (in.) vs 1000–500-mb thickness (dm) values at the observed location of heavy rainfall. Each plotted number on the graph represents the category assigned to the precipitation event based on the areal coverage of the 3 in. or more precipitation (defined in Table 1). The line depicted in the diagram represents a thickness and precipitable water value plotted from the table presented by Funk (1991), i.e., a 70% saturation line.

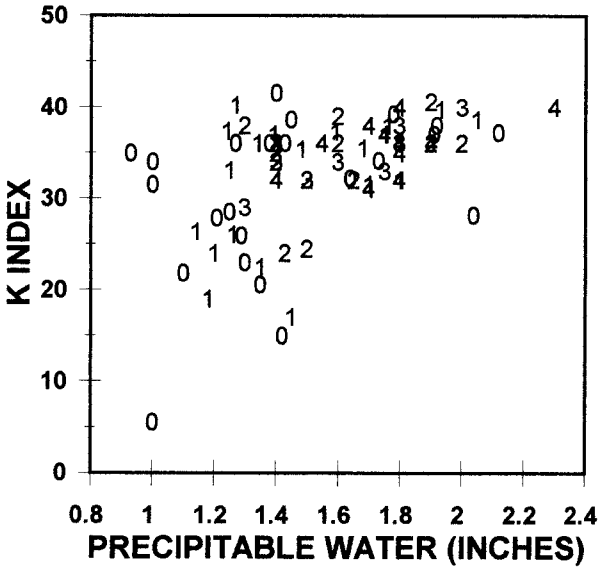

FIG. 7. Scatter diagram for *K* index and precipitable water (in.) Each plotted number on the graph represents the category assigned to the precipitation event based on the areal coverage of the 3 in. or more precipitation (defined in Table 1).

ration thickness as the geopotential thickness of a saturated column of air associated with a given precipitable water value. Funk (1991) noted that HPC synopticians empirically determined that organized heavy convective rainfall typically was associated with 70% or greater mean relative humidity (assuming a standard atmosphere) and he referred to this as the saturated thickness. To minimize the confusion that might arise from the different definitions of saturated thickness given by Swayne and Funk, henceforth, the Funk definition will be referred to as the *70% saturation thickness.*

To examine whether there is a relationship between the 70% saturation thickness and where an organized convective system is most likely to develop, values of precipitable water were plotted versus 1000–500-mb thickness at the time nearest the start of each MCS (Fig. 6). The line on the diagram is plotted using the table provided by Funk (1991) for the 70% saturation thickness. Along and to the right of the line in Fig. 6, the mean relative humidity of the column is 70% or higher (assuming a standard atmosphere). Most of the category 3 and 4 events occurred along or to the right of the line and were associated with higher mean relative humidity than the category 0 and 1 events. The scale and intensity of rainfall associated with convective systems at least in part seemed to be modulated by the mean relative humidity of the 1000–500-mb layer. Some smaller-scale, less extreme events, however, also occurred with high precipitable water and mean relative humidity above 70% indicating that other factors also modulate the scale of a system. Regardless of category, the core of the heaviest rainfall usually fell within the axis of highest relative humidity.

The fact that all larger-scale events were found near or to the right of the line in Fig. 6 may explain why forecasters at HPC have been able to use the 70% saturation thickness table presented by Funk with some confidence. The technique allows forecasters to recognize when a larger-scale, heavy convective rainfall event may be more likely. Even though heavy rainfall events sometimes occur with the lower relative humidity found to the left of the line (Fig. 6), they usually occur on a smaller scale (i.e., categories 0 and 1) that may be too small for a forecaster to be able to predict accurately.

Funk (1991) also noted that HPC forecasters routinely use precipitable water and *K* index values as indicators of the potential for heavy rainfall. The precipitable water and *K* index values for the category 3 and 4 events averaged 1.64 in. and 35, respectively, at the location where the heaviest rainfall subsequently was observed. By contrast, the mean precipitable water and *K* index for the two lightest categories (category 0 and 1) averaged 1.46 in. and 30, respectively. Despite the differences in the mean values between the most and least extreme events, some category 0 and 1 events occurred with higher precipitable water and *K* index values than observed with some of the category 3 and 4 cases (Fig. 7). Therefore, moisture and instability were not adequate to differentiate between categories. Also, the location of the heavy rainfall was centered in, but on the north side of, the axis of highest precipitable water values, regardless of category.

Forecasters at HPC and the Storm Prediction Center have long used 700-mb temperatures of 12°C or warmer

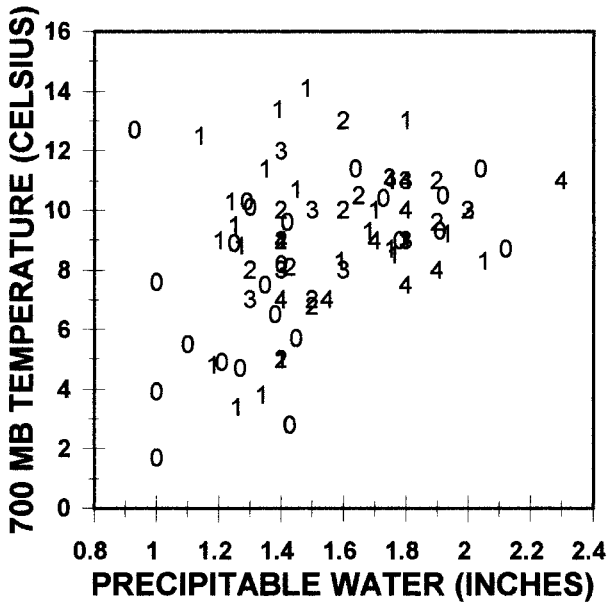

FIG. 8. Same as Fig. 7 except 700-mb temperature (°C) replaces 1000–500-mb thickness along the *y* axis.

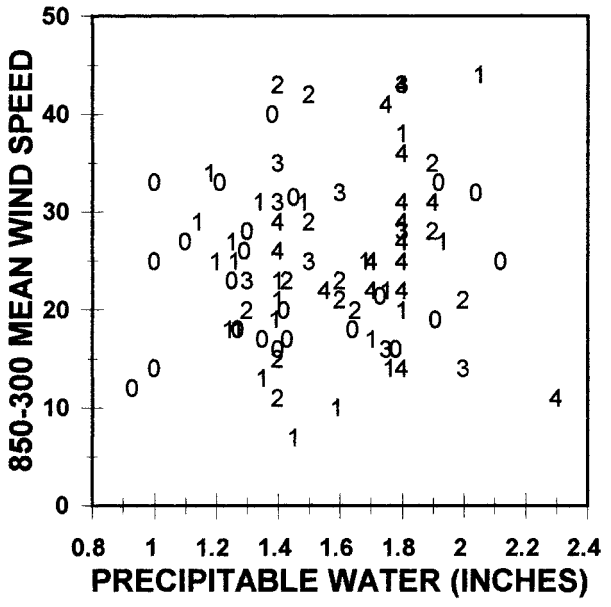

FIG. 9. Same as Fig. 7 except the *y* axis has been changed to 850–300-mb mean wind speed ($|V_{CL}|$, kt), where the mean wind speed is found using $|V_{CL}| = |(V_{850} + V_{700} + V_{500} + V_{300})/4|$.

as an indicator that a strong cap generally would inhibit the development of a convective system. The reason this second rule of thumb works appears to be related to scale. In this study, no larger-scale, extreme convective heavy rainfall events (i.e., categories 3 and 4) occurred at temperatures above 12°C (Fig. 8). However, a few smaller-scale, less intense ones did occur. Glass and Ferry (1995) also found that none of their eight cases of convective heavy rainfall developed where there were high ambient 700-mb temperatures. Convective inhibition (CIN), a more accurate measure of the work per unit mass required to break a cap (Bluestein and Jain 1985), was not evaluated because it was unavailable via the RDAS dataset.

As mentioned earlier, researchers (e.g., Merritt and Fritsch 1984; Corfidi et al. 1996) have shown that the mean wind from 850 to 300 mb gives a good approximation of the speed and direction of movement of individual convective cells. Our data suggests that neither precipitable water nor mean wind speed can be used by themselves to discriminate the most likely scale and intensity of an event (Fig. 9). One possible reason for weak correlation with the mean wind may be that the net movement of a convective system is a result of cell movement and system propagation (Chappell 1986). Satellite imagery for these events suggested the larger-scale heavy rainfall events were often produced by a steady stream of regenerating convective cells moving along a stationary low-level boundary. Individual cells may be relatively fast moving, but the general area of convective and stratiform rains associated with the more extreme MCSs were slow moving because new cells formed upstream.

The data also suggest that heavy-to-extreme rainfall events can occur with much less vertical wind speed shear than is usually associated with most other severe weather threats (i.e., high surface winds, tornadoes, and hail). For example, the category 4 event on the far right-hand side of Fig. 9 occurred with weak mean flow implying that only weak vertical speed shear was present. However, the winds veered considerably with height, especially at low levels. This is consistent with Maddox et al. (1979), who noted that considerable veering of the low-level winds but only weak-to-moderate deep-layered shear were present where most MCSs formed. This shear profile is consistent with MCS formation along or north of a low-level boundary.

The larger-scale heavy rainfall events that did occur with higher mean wind speeds (not shown) also were associated with stronger 850-mb winds and moisture transport. This is not surprising since the amount of rainfall produced by a convective system is related to the cell movement and propagation rate in which new cells develop along the flank of the storm (Doswell et al. 1996). Corfidi et al. (1996) have shown that the direction and speed of an MCS is modulated by the low-level jet. When the direction and speed of the low-level jet approaches that of the mean wind, a slow moving or quasi-stationary convective system is more likely. Detailed study of two of the 6 in. or greater rainfall events in our dataset supports this explanation (Junker and Schneider 1997).

In summary, the main differences between the most (category 3 and 4) and least extreme (category 0 and 1) events were 1) the strength of the warm advection, 2) the 1000–500-mb mean relative humidity, 3) the breadth of the axis of stronger values of moisture trans-

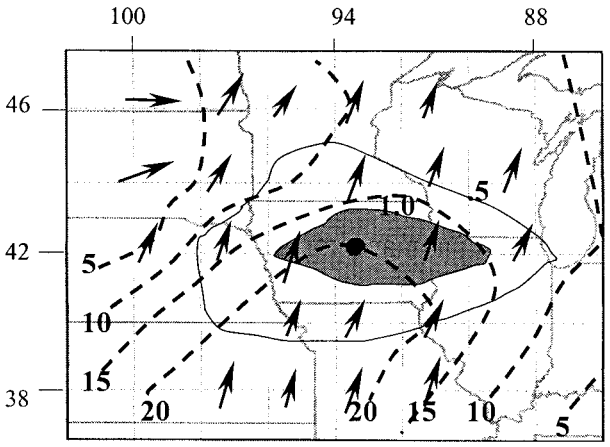

FIG. 10. Composite of 850-mb wind direction (arrows), isotachs (dashed, contour interval = 5 kt), and temperature advection (solid line depicts values $\geq 0.5 \times 10^{-4}$ K s^{-1} and shaded area depicts values $\geq 1.0 \times 10^{-4}$ K s^{-1}) for the 12 cases with the largest areal coverage of 3 in. or greater rainfall (category 4). The grid spacing is 2° lat by 2° long and is centered on the location of the center of the heaviest observed isohyet. The composite has been normalized to a point in Iowa (the small black circle).

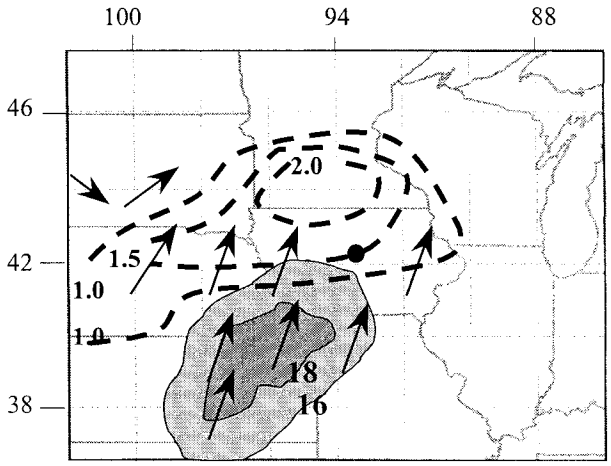

FIG. 11. Same as in Fig. 10 except for magnitude and direction of 850-mb moisture flux (light shaded area represents the magnitudes $\geq 16 \times 10^{-2}$ m s^{-1} and dark shaded area values $\geq 18 \times 10^{-2}$ m s^{-1}; the arrows represent the direction of the moisture flux vector) and 850-mb moisture flux convergence. The magnitude of the moisture flux convergence is shown for values $\geq 1.0 \times 10^{-7}$ m s^{-1} contoured every 0.5×10^{-7} m s^{-1}.

port feeding northward into the low-level boundary, and 4) the length of the low-level moisture flux convergence that was aligned along the mean flow upstream from the location of the rainfall maximum. The latter finding suggests that propagation plays an important role in modulating the scale and intensity of rainfall events.

Subjective evaluation comparing category 3 and 4 with category 0 and 1 events suggested that the location where the strongest low-level moisture transport and moisture flux convergence and instability was located with respect to the initial convection also was important. The strongest low-level moisture convergence was more often found upstream from the initial convective cells in category 3 and 4 events than in category 0 and 1 cases. In addition, the axis of strongest low-level winds and moisture transport seemed to translate eastward more slowly during the most extreme cases, again emphasizing the importance of propagation.

4. Composites

Examination of the composite fields of the 12 most extreme of the category 4 events illustrates some of the key features of the synoptic climatology for extreme rainfall events. The heavy rain usually was centered along the axis of strongest 850-mb winds but slightly north of the wind maximum (Fig. 10). This was true for all categories in this study, as well as for the synoptic-, frontal-, and mesohigh-type flash flood events studied by Maddox et al. (1979). Composites by Augustine and Caracena (1994) documenting the precursor conditions of nocturnal MCS development also indicated that initiation usually occurred north of the low-level jet as defined by the surface geostrophic wind maximum.

The composite maximum rainfall also was located just northeast (downwind) of an axis of strong 850-mb moisture flux in a region of 850-mb moisture flux convergence (Fig. 11). However, the strongest 850-mb moisture flux convergence was located north and west of where the heaviest rainfall subsequently was observed. This observation probably can be attributed to two factors: 1) the initial convection likely was rooted in the boundary layer in the early stages of most events near the zone of surface convergence but south of the 850-mb convergence, and 2) the initial convection likely formed west of the observed rainfall maximum and then shifted eastward with the mean flow. To test the validity of these factors, 982-mb sigma-level data was available for subjective evaluation and Rapid Update Cycle surface analyses (Benjamin et al. 1994) were available for detailed examination of 2 of the 12 most extreme events. Both the subjective evaluation and the more detailed examination of the two heavy rainfall events (Junker and Schneider 1997) give credence to these two arguments. In both cases, surface moisture convergence developed upstream from the initial convection prior to a period of backbuilding convection. In addition, earlier studies (Hudson 1971; Doswell 1985) noted that development of surface moisture convergence usually precedes convective initiation, making it a useful forecast tool.

The composites also support the idea that MCSs associated with heavy rains often develop near or just downwind from an axis of high 850-mb equivalent potential temperature (θ_e) in an area of positive θ_e advection (Fig. 12). However, the center of the heavy rain usually was found on the north or northeast side of the maximum θ_e values and just south of the maximum θ_e

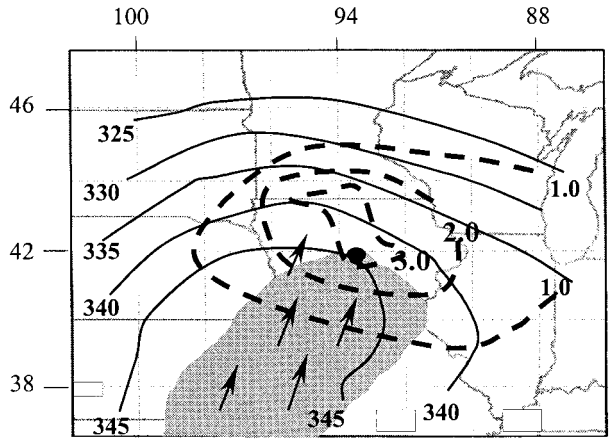

FIG. 12. Same as Fig. 10 except for 850-mb wind direction (arrows) and isotachs (shaded area ≥20 kt), equivalent potential temperature (solid lines, interval = 5 K), and advection of equivalent potential temperature by the wind (dashed lines, values ≥1 × 10^{-4} K s^{-1} are contoured with a contour interval of 1 × 10^{-4} K s^{-1}).

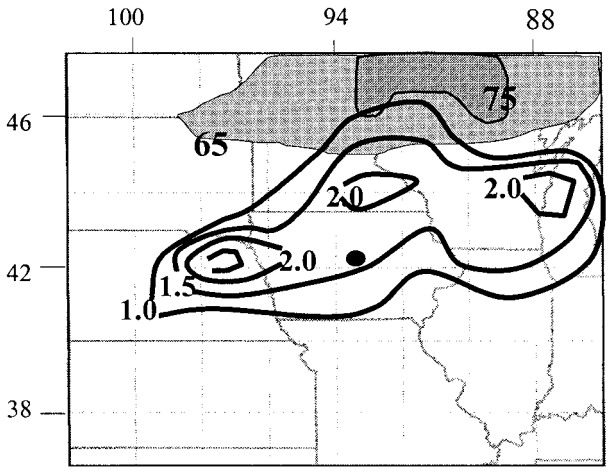

FIG. 13. Same as Fig. 10 except for the analysis is of 250-mb isotachs (shaded values are ≥65 kt, contoured every 10 kt) and 250-mb divergence (bold lines, values shown are ≥1.0 × 10^{-5} s^{-1} with a contour interval of 0.5 × 10^{-5} s^{-1}).

advection. Subjective evaluation indicated this was true for most cases within each category. Glass and Ferry (1995) found a similar pattern present for a smaller dataset.

An area of 850-mb warm advection also was collocated with the heavy rainfall events (Fig. 10). However, for the most extreme cases, the strength of the thermal advection was weaker than the θ_e advection because the temperature gradient usually was not as strong as the θ_e gradient. This suggested that strong moisture advection was present. However, both fields gave a clear signal that could be used to predict where the heaviest rainfall was likely to fall for the majority of cases within each category.

A composite of the 250-mb wind field (Fig. 13) placed the maximum rainfall associated with the 12 most extreme of the 15 total category 4 events roughly in the right-rear entrance region of a jet streak. Individually, 83% of these 12 cases were associated with upper-level divergence that was clearly defined within the right entrance region of a straight or anticyclonically curved jet streak. This higher percentage than was found for the entire set of all cases (60%) may be a reflection of the small dataset, but may also reflect that the largest, most extreme events were associated with stronger dynamics. Kane et al. (1987) found that synoptic- and frontal-type heavy rainfall events typically were of larger scale than mesohigh-type events and suggested that they were associated with stronger dynamics than mesohigh events.

The fact that a broad area of 250-mb divergence was present during the most extreme events, therefore, is not unexpected (Fig. 13). However, forecasters should note that the location of the heaviest rainfall usually was found in the gradient south of the maximum values of 250-mb divergence. This finding is probably related to sloped ascent (isentropic lift) that is taking place as potentially unstable parcels are lifted from south to north along a boundary toward the upper-level divergence associated with the entrance region of a jet streak. Given sufficient moisture and lift, the parcels may release their instability before reaching the location beneath the upper-level divergence maximum, potentially resulting in the heaviest rain to the south of the area of maximum divergence aloft.

5. Conclusions

The findings of this study suggest there are factors that make extreme rainfall events more likely. However, the differences in the synoptic and mesoscale patterns between category 4 (the most extreme) and category 0 events were subtle. We have defined extreme events based on the areal size of the 3 in. or greater isohyet, a rather arbitrary definition. Even using this criteria, no single factor could be relied upon to determine if a convective rainfall event would be an extreme one. Instead, a number of factors appear to determine the scale and intensity of a rainfall event. Many of these factors are discussed in the Doswell et al. (1996) ingredients-based methodology for flash flood forecasting. They note that the heaviest precipitation occurs where the rainfall rate is highest for the longest time. Furthermore, the duration of a high precipitation rate at any location is dependent on system movement, system size, and within-system variations in rainfall intensity.

This study also utilized the Doswell et al. approach for data analysis and appears to confirm that the following factors govern whether a convective event becomes extreme: 1) slow system movement, 2) prolonged heavy-to-intense rainfall rates, and 3) areal coverage of intense rainfall rates. Most of the extreme events were associated with a surface boundary aligned roughly parallel to the mean flow. Such an alignment increases the chances of cell training along the boundary. Because of

the short lifetime of individual cells, most of the extreme events were produced by cells regenerating upstream and then tracking with the mean flow over the same general area, thereby prolonging the period of heavy rainfall.

The breadth, location, and movement of the axis of stronger moisture flux values appeared to play a role in modulating the rainfall. A broader axis feeding into the boundary likely produces a larger area of moderate-to-strong moisture flux convergence, which may increase the area where convection will develop. The strongest low-level moisture flux convergence and instability for the most extreme events usually were located along the western edge of the organizing convection. In addition, subjective evaluation suggested that the axis of strongest low-level winds and moisture flux translated downstream more slowly during the most extreme cases. Therefore, cell regeneration occurred upstream of the parent MCS (i.e., a backward propagation vector), which prolonged the period of heavy rainfall and caused several of the convective systems to become quasi-stationary.

Available moisture also appeared to modulate the scale of the events. The category 3 and 4 events were associated with higher mean precipitable water and relative humidity values than category 0 or 1 events. Doswell et al. (1996) noted the importance of precipitation efficiency (the ratio of the mass of water falling as precipitation to the mass of water vapor entering the cloud) in determining rainfall rates. They noted that environmental relative humidity is a key factor in determining the amount of liquid water in the cloud that evaporates, and that lower (higher) environmental relative humidity leads to more (less) evaporation through entrainment. Therefore, the higher mean 1000–500-mb relative humidities associated with the category 3 and 4 events apparently promoted higher rainfall efficiency within the convective systems.

There did appear to be some forecast utility for several of the rules of thumb practiced by the forecasters at HPC. For example, most category 3 and 4 events occurred at 1000–500-mb thicknesses that were at least 70% saturated. No category 3 or 4 events occurred at 700-mb temperatures above 12°C, although a few smaller-scale events did occur. The temperature at 700 mb appears to be a decent first guess in estimating the strength of the cap. However, forecasters are encouraged to examine soundings and the CIN since it measures the actual work needed to break the cap.

The small scale of the core of heaviest rainfall within the extreme convective events, many of which produced severe flash flooding, argues for a probabilistic approach to forecasting flash flooding. This study suggests that forecasters may be able to develop some skill in predicting when an extreme event is likely, but they probably would not be able to predict the precise location with the accuracy needed to determine which river basin or subbasin would flood with much lead time. A more realistic approach might be to predict the probability of occurrence of various size areas of 3, 4, or 5 in. or greater rainfall within a predefined region over a specified time period (i.e., 12 or 24 h). Such an approach would provide information about the uncertainty of the scale and location of the core of heavy rains that are associated with flash floods.

Acknowledgments. The authors would like to thank Mr. David Reynolds, Mr. Edwin Danaher, Mr. Pete Manousis, Mr. Ted Funk, and one anonymous reviewer for their helpful reviews of the manuscript. The authors also would like to thank Dr. Roderick Scofield for providing satellite imagery for the study.

REFERENCES

Augustine, J. A., and F. Caracena, 1994: Lower-tropospheric precursors to nocturnal MCS development over the central United States. *Wea. Forecasting,* **9,** 116–135.

Bartels, D. L., and A. A. Rockwood, 1983: Internal structure and evolution of a dual mesoscale convective complex. Preprints, *Fifth Conf. on Hydrometeorology*, Tulsa, OK, Amer. Meteor. Soc., 97–102.

Bell, G. D., and J. E. Janowiak, 1995: Atmospheric circulation associated with the Midwest floods of 1993. *Bull. Amer. Meteor. Soc.,* **76,** 681–695.

Benjamin, S. G., K. L. Brundage, and L. L. Morone, 1994: The Rapid Update Cycle. Part I: Analysis/model description. Tech. Procedures Bull. 416, NOAA/NWS, 16 pp. [Available from National Weather Service, Office of Meteorology, 1325 East–West Highway, Silver Spring, MD 20910.]

Bluestein, H. B., and M. H. Jain, 1985: Formation of mesoscale lines of precipitation: Severe squall lines in Oklahoma during the spring. *J. Atmos. Sci.,* **42,** 1711–1734.

Chappell, C., 1986: Quasi-stationary convective events. *Mesoscale Meteorology and Forecasting,* P. S. Ray, Ed., Amer. Meteor. Soc., 289–310.

Corfidi, S. F., J. H. Merritt, and J. M. Fritsch, 1996: Predicting the movement of mesoscale convective complexes. *Wea. Forecasting,* **11,** 41–46.

Dimego, G. J., K. E. Mitchell, R. A. Petersen, J. E. Hoke, G. P. Gerrity, J. J. Tuccillo, W. L. Wobus, and H. H. Ming, 1992: Changes to NMC's Regional Analysis and Forecast System. *Wea. Forecasting,* **7,** 185–198.

Doswell, C. A., III, 1985: *The Operational Meteorology of Convective Weather. Vol. II: Storm Scale Analysis.* NOAA—Environmental Sciences Group, 240 pp. [Available from Storm Prediction Center, 1313 Halley Circle, Norman, OK 73069.]

——, H. E. Brooks, and R. A. Maddox, 1996: Flash flood forecasting: An ingredients-based methodology. *Wea. Forecasting,* **11,** 560–581.

Fritsch, J. M., R. J. Kane, and C. R. Chelius, 1986: The contribution of mesoscale convective systems to the warm season precipitation in the United States. *J. Appl. Meteor.,* **25,** 1333–1345.

Funk, T. W., 1991: Forecasting techniques utilized by the Forecast Branch of the National Meteorological Center during a major convective rainfall event. *Wea. Forecasting,* **6,** 548–564.

Glass, F. H., and D. L. Ferry, 1995: Characteristics of heavy rainfall events across the mid-Mississippi Valley during the warm season: Meteorological conditions and a conceptual model. Preprints, *14th Conf. on Weather Analysis and Forecasting,* Dallas, TX, Amer. Meteor. Soc., 34–41.

Guttman, N. B., J. R. M. Hosking, and J. R. Wallis, 1994: The 1993 Midwest extreme precipitation in historic and probabilistic perspective. *Bull. Amer. Meteor. Soc.,* **75,** 1785–1792.

Hudson, H. R., 1971: On the relationship between horizontal moisture

convergence and convective cloud formation. *J. Appl. Meteor.*, **10,** 755–762.

Junker, N. W., and R. S. Schneider, 1997: Two case studies of quasi-stationary convection during the 1993 Great Midwest Flood. *Natl. Wea. Dig.*, **21,** 5–17.

Juring, X., and R. A. Scofield, 1989: Satellite-derived rainfall estimates and propagation characteristics associated with mesoscale convective systems (MCSs). NOAA/NESDIS Tech. Memo. NESDIS 25, Washington, DC, 49 pp. [Available from National Environmental Satellite Data and Information Service, Rm. 703, 5200 Auth Rd., Camp Springs, MD 20746.]

Kane, R. B., Jr., C. R. Chelius, and J. M. Fritsch, 1987: Precipitation characteristics of mesoscale weather systems. *J. Climate Appl. Meteor.*, **26,** 1345–1357.

Kocin, P. J., L. W. Uccellini, and R. A. Petersen, 1986: Rapid evolution of a jet streak circulation in a pre-convective environment. *Meteor. Atmos. Phys.*, **35,** 103–138.

Konrad, C. E., II, 1997: Synoptic features associated with warm season heavy rainfall over the interior southeastern United States. *Wea. Forecasting,* **12,** 557–571.

Kunkel, K. E., S. A. Changnon, and J. R. Angel, 1994: Climatic aspects of the 1993 upper Mississippi River basin flood. *Bull. Amer. Meteor. Soc.*, **75,** 811–822.

Lowry, D. A., 1972: Climatological relationships among precipitable water, thickness, and precipitation. *J. Appl. Meteor.*, **11,** 1326–1333.

Maddox, R. A., 1980: Mesoscale convective complexes. *Bull. Amer. Meteor. Soc.*, **61,** 1374–1387.

——, 1983: Large-scale meteorological conditions associated with midlatitude mesoscale convective complexes. *Mon. Wea. Rev.*, **111,** 1475–1493.

——, C. F. Chappell, and L. R. Hoxit, 1979: Synoptic and mesoscale aspects of flash flood events. *Bull. Amer. Meteor. Soc.*, **60,** 115–123.

——, D. M. Rogers, and K. W. Howard, 1982: Mesoscale complexes over the United States during 1981—Annual summary. *Mon. Wea. Rev.*, **110,** 1501–1514.

McAnelly, R. L., and W. R. Cotton, 1986: Meso-β-scale characteristics of an episode of meso-α-scale convective complexes. *Mon. Wea. Rev.*, **114,** 1740–1770.

Merritt, J. H., and J. M. Fritsch, 1984: On movement of heavy precipitation areas of midlatitude mesoscale convective complexes. Preprints, *10th Conf. on Weather Analysis and Forecasting,* Clearwater, FL, Amer. Meteor. Soc., 529–536.

NOAA, 1994: Natural disaster survey report: The Great Flood of 1993. National Oceanic and Atmospheric Administration, 128 pp. [Available from U.S. Dept. of Commerce, National Weather Service, 1325 East–West Highway, Silver Spring, MD 20910.]

Newton, C. W., and S. Katz, 1958: Movement of large convective rainstorms in relation to the winds aloft. *Bull. Amer. Meteor. Soc.*, **39,** 129–136.

Olson, D. A., N. W. Junker, and B. Korty, 1995: Evaluation of 33 years of quantitative precipitation forecasting at the NMC. *Wea. Forecasting,* **10,** 498–511.

Shi, J., and R. A. Scofield, 1987: Satellite-observed mesoscale convective systems (MCSs) propagations and a 3–12-hour heavy precipitation index. NOAA/NESDIS Tech. Memo. 20, Washington, DC, 43 pp. [Available from National Environmental Satellite Data and Information Service, Rm. 703, 5200 Auth Rd., Camp Springs, MD 20746.]

Swayne, W. W., 1956: Quantitative analysis and forecasting of winter rainfall patterns. *Mon. Wea. Rev.*, **84,** 53–65.

Uccellini, L. W., and D. R. Johnson, 1979: The coupling of upper- and lower-tropospheric jet streaks and implications for the development of severe convective storms. *Mon. Wea. Rev.*, **107,** 682–703.